2011 International Symposium on Nonlinear Theory and its Applications
NOLTA2011, Kobe, Japan, September 4-7, 2011

Basic Analysis of Generalized Asynchronous Digital Spiking Neuron Model

Takashi Matsubara† and Hiroyuki Torikai†

†Graduate School of Engineering Science, Osaka University
1-3 Machikaneyama Toyonaka, Osaka, 560-8531 Japan

Abstract—A generalized asynchronous digital spiking neuron model that can be implemented by an asynchronous sequential logic circuit is introduced. The model is the most generalized version of asynchronous sequential logic circuit based neurons, where the sensitivity of its vector field to a stimulation input is generalized. It is clarified that the GDN can exhibit various bifurcations observed in some standard ODE neuron models.

1. Introduction

Various spiking neuron models suited for electronic circuit implementations have been proposed so far, where there exist two major approaches: (i) an analog approach that implements a nonlinear *ordinary differential equation* (ab. ODE) in an analog nonlinear circuit [1–4], and (ii) a digital approach that implements a numerical integration in a digital processor [5–7]. Recently, an alternative hardware-oriented neuron modeling approach has been proposed, where a nonlinear dynamics of a neuron is modeled by an asynchronous cellular automaton that is implemented by an asynchronous sequential logic circuit [8–11]. In this paper, a *generalized asynchronous digital spiking neuron model* (ab. GDN) is introduced, where the sensitivity of its vector field to a stimulation input is generalized. The GDN consists of registers, logic gates, and reconfigurable wires, where the pattern of the wires is a control parameter that determines the nonlinear dynamics of the GDN. In this paper, it is clarified that the GDN can exhibit various bifurcations (e.g., supercritical Hopf bifurcation, saddle-node bifurcation) that are also observed in some standard ODE neuron models [12]

2. Generalized asynchronous digital spiking neuron

In this section, a *generalized asynchronous digital spiking neuron model* (ab. GDN), whose diagram is shown in Fig. 1, is introduced. The GDN has the following four registers. (1) The *membrane register* is an N-bit bi-directional shift register having an integer state $V \in \mathbf{Z}_N \equiv \{0, \cdots, N-1\}$ encoded by the one-hot coding manner, where "≡" denotes "is defined by". From a neuron model viewpoint, the state V can be regarded as a *membrane potential*. (2) The *recovery register* is an M-bit bi-directional shift register having an integer state $U \in \mathbf{Z}_M \equiv \{0, \cdots, M-1\}$ encoded by the one-hot coding manner. From a neuron model viewpoint, the state U can be regarded as a *recovery variable*. (3) The *membrane velocity counter* is a K-bit register having an integer state $P \in \mathbf{Z}_K \equiv \{0, \cdots, K-1\}$ encoded by the thermometer coding manner. The state P controls a velocity of the membrane potential V. (4) The *recovery velocity counter* is a J-bit register having an integer state $Q \in \mathbf{Z}_J \equiv \{0, \cdots, J-1\}$ encoded by the thermometer coding manner. The state Q controls a velocity of the recovery variable U. The states V, U, P and Q are clamped to the range $[0, N-1]$, $[0, M-1]$, $[0, K-1]$ and $[0, J-1]$, respectively. As shown in Fig. 1, the registers and the counters are connected to each other via the following two memoryless units. (i) The *vector field unit* consists of logic gates and reconfigurable wires. This unit determines the characteristics of a vector field of the states (V, U) as its name implies. (ii) The *reset value unit* consists of logic gates and reconfigurable wires. From a neuron model viewpoint, this unit determines values to which the states (V, U) are reset when the GDN fires, as its name implies. The GDN accepts a periodic *internal clock* $Clk(t)$ described by

$$Clk(t) = \begin{cases} 1 & \text{if } t \pmod 1 = 0, \\ 0 & \text{otherwise,} \end{cases}$$

where $t \in [0, \infty)$ is a continuous time. In the next subsection *A*, autonomous behaviors of the GDN (i.e., behaviors when no stimulation input spike-train $Stm(t)$ is applied) are investigated. After that, in the subsection *B*, non-autonomous behaviors of the GDN (i.e., behaviors when a stimulation input spike-train $Stm(t)$ is applied) are investigated.

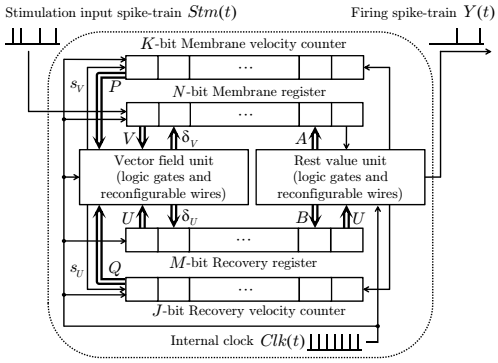

Figure 1: Generalized asynchronous digital spiking neuron model (ab. GDN).

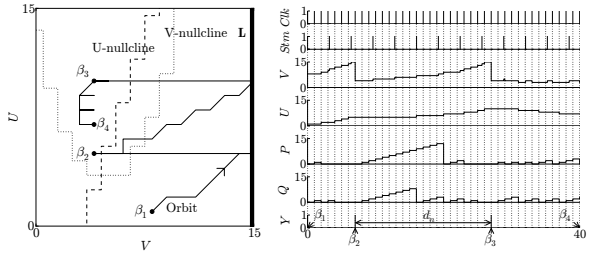

Figure 2: A phase plane and state transitions. V-nullcline (U-nullcline) is a border between $D_V \in \{-1, 0\}$ and $D_V = 1$ ($D_U \in \{-1, 0\}$ and $D_U = 1$). The bit lengths of the registers and the counters are $N = M = K = J = 16$. The parameters are $\mathbf{\Gamma} = (7, 0.3, 0.2, 3, 0.1, 16, 0.5, 0.3, 0)$ defined in (5). A periodic stimulation input spike-train $Stm(t)$ with a frequency 0.312 via the synaptic weight $W = 1$ is applied to the GDN.

2.1. Autonomous behaviors

Let us begin with defining the following subset $\mathbf{L}$ in the state space $\mathbf{Z}_N \times \mathbf{Z}_M$ (see also Fig. 2).

$$\mathbf{L} \equiv \{(V, U) | V = N - 1, U \in \mathbf{Z}_M\} \subset \mathbf{Z}_N \times \mathbf{Z}_M.$$

From a neuron model viewpoint, $\mathbf{L}$ can be regarded as a *firing threshold*.

First, let us consider the case of $(V, U) \notin \boldsymbol{L}$. In this case, the vector field unit shown in Fig. 1 triggers the transitions of the states (P, Q) of the velocity counters and the states (V, U) of the registers by generating signals $(s_V, s_U) \in \{0, 1\}^2$ and $(\delta_V, \delta_U) \in \{-1, 0, 1\}^2$ as follows.

$$\begin{aligned}
P(t^+) &= \begin{cases} P(t) + 1 & \text{if } s_V(t) = 0, Clk(t) = 1, \\ 0 & \text{if } s_V(t) = 1, Clk(t) = 1, \\ P(t) & \text{otherwise,} \end{cases} \\
Q(t^+) &= \begin{cases} Q(t) + 1 & \text{if } s_U(t) = 0, Clk(t) = 1, \\ 0 & \text{if } s_U(t) = 1, Clk(t) = 1, \\ Q(t) & \text{otherwise,} \end{cases} \\
V(t^+) &= \begin{cases} V(t) + \delta_V & \text{if } Clk(t) = 1, \\ V(t) & \text{otherwise,} \end{cases} \\
U(t^+) &= \begin{cases} V(t) + \delta_V & \text{if } Clk(t) = 1, \\ V(t) & \text{otherwise,} \end{cases}
\end{aligned} \tag{1}$$

where the velocity counters accept the internal clock $Clk(t)$ and the signals (s_V, s_U), and the registers accept the signals (δ_V, δ_U) from the vector field unit. The signals (s_V, s_U) and (δ_V, δ_U) are generated as follows.

$$s_V = \begin{cases} 1 & \text{if } P \geq P_h(V, U), \\ 0 & \text{if otherwise,} \end{cases}, s_U = \begin{cases} 1 & \text{if } Q \geq Q_h(V, U), \\ 0 & \text{if otherwise,} \end{cases}$$

$$\delta_V = \begin{cases} \mathrm{sgn}(\mathcal{F}(V, U)) & \text{if } P \geq P_h(V, U), \\ 0 & \text{otherwise,} \end{cases}$$

$$\delta_U = \begin{cases} \mathrm{sgn}(\mathcal{G}(V, U)) & \text{if } Q \geq Q_h(V, U), \\ 0 & \text{otherwise,} \end{cases}$$

where the signum function $\mathrm{sgn}(x)$ gives the sign of a real number x and the functions $\mathcal{F}(V, U)$, $\mathcal{G}(V, U)$, $P_h(V, U)$ and $Q_h(V, U)$ are defined as follows.

$$\begin{aligned}
\mathcal{F}(V, U) &= N(\gamma_1 (V/N - \gamma_2)^2 + \gamma_3 - U/M)/\lambda, \\
\mathcal{G}(V, U) &= \mu M(\gamma_4 (V/N - \gamma_2) + (\gamma_3 + \gamma_5) - U/M)/\lambda, \\
P_h(V, U) &= \lfloor |\mathcal{F}^{-1}(V, U)| \rfloor - 1, \\
Q_h(V, U) &= \lfloor |\mathcal{G}^{-1}(V, U)| \rfloor - 1,
\end{aligned}$$

where $(\gamma_1, \gamma_2, \gamma_3, \gamma_4, \gamma_5, \lambda, \mu)$ are parameters, the function $\lfloor x \rfloor$ gives the integer part of a real number x, and $P_h(V, U)$, $Q_h(V, U)$ are clamped to the range $[0, K - 1]$, $[0, J - 1]$, respectively.

Second, let us consider the case of $(V, U) \in \mathbf{L}$. In this case, the reset value unit shown in Fig. 1 triggers the transitions of the states (P, Q) of the velocity counters and the states (V, U) of the registers by generating integer signals $(A, B) \in \mathbf{Z}_N \times \mathbf{Z}_M$ encoded by the one-hot coding manners, as follows.

$$\begin{aligned}
&(P(t^+), Q(t^+), V(t^+), U(t^+)) = \\
&\begin{cases} (0, 0, A(t), B(t)) & \text{if } (V, U) \in \mathbf{L}, Clk(t) = 1, \\ (P(t), Q(t), V(t), U(t)) & \text{otherwise,} \end{cases}
\end{aligned} \tag{2}$$

where the signals (A, B) are generated as follows.

$$A = \lfloor \rho_1 N \rfloor, \quad B(U) = U + \lfloor \rho_2 M \rfloor,$$

where (ρ_1, ρ_2) are parameters and $A, B(U)$ are clamped to the range $[0, N - 1]$, $[0, M - 1]$, respectively. Repeating the firing resets, the GDN generates the following *firing spike-train* $Y(t)$.

$$Y(t) = \begin{cases} 1 & \text{if } (V(t), U(t)) \in \mathbf{L}, Clk(t) = 1, \\ 0 & \text{otherwise.} \end{cases} \tag{3}$$

2.2. Non-autonomous behaviors

Let us now apply the following stimulation input spike-train $Stm(t)$ to the GDN.

$$Stm(t) = \begin{cases} W & \text{if } t = t_1, t_2, \cdots, \\ 0 & \text{otherwise,} \end{cases}$$

where $t = t_1, t_2, \cdots$ are input spike positions and $W \in \{-1, 1\}$ is a parameter. From a neuron model viewpoint, the stimulation input spike $Stm(t)$ can be regarded as a *stimulation input* and W can be regarded as a *synaptic weight*. A post-synaptic stimulation spike $Stm = W$ induces a transition of the membrane potential V as follows.

$$V(t^+) = \begin{cases} V(t) + W & \text{if } Stm(t) = W, \\ V(t) & \text{otherwise.} \end{cases} \tag{4}$$

Fig. 2 shows basic non-autonomous behaviors of the GDN.

As a result, the dynamics of the GDN is described by (1)–(4), and is characterized by the following parameters.

$$N, M, K, J, \mathbf{\Gamma} = (\gamma_1, \gamma_2, \gamma_3, \gamma_4, \gamma_5, \lambda, \mu, \rho_1, \rho_2). \tag{5}$$

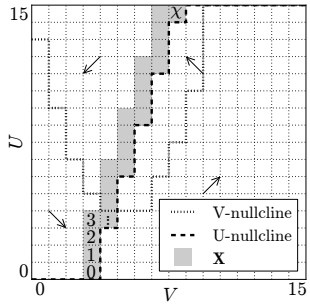

Figure 3: Definitions of the subset $\mathbf{X}$ in Eq. (6) and its co-ordinate X in Eq. (7).

3. Bifurcation Diagrams

In this section, it is shown that the GDN can exhibit various bifurcations . For simplicity, we focus on the following periodic stimulation input spike-train $Stm(t)$.

$$Stm(t) = \begin{cases} W & \text{if } (t+\theta_0) \pmod{f_S^{-1}} = 0, \\ 0 & \text{otherwise,} \end{cases}$$

where f_S is an input frequency, $\theta_0 \in [0, f_S^{-1})$ is an initial input phase, and a *post-synaptic stimulation* I to the GDN is defined as $I = f_S \times W$. To create bifurcation diagrams, let us define the following subset $\mathbf{X}$ of the state space $\mathbf{Z}_N \times \mathbf{Z}_M$ as shown in Fig. 3.

$$\mathbf{X} \equiv \left\{ (j,i) \;\middle|\; \begin{array}{l} (j,i) \in \mathbf{Z}_N \times \mathbf{Z}_M,\ D_U(j,i) \neq 1, \\ (j,i) \text{ has at least one 8-neighbor} \\ (l,k) \text{ at which } D_U(l,k) = 1 \end{array} \right\}. \quad (6)$$

As shown in Fig. 3, the subset $\mathbf{X}$ is indexed by an integer

$$X \in \mathbf{Z}_X \equiv \{0, 1, \cdots, \chi\} \quad (7)$$

encoded by the chain coding manner, where χ is an integer determined by the parameters $(N, M, K, J, \mathbf{\Gamma})$. Fig. 4 shows the bifurcation diagrams for X with respect to a post-synaptic stimulation I.

In Fig. 4(a1), the left plots (arrow α_1) correspond to stable equilibrium sets (i.e., resting states) and the right plots (arrow α_2) correspond to stable limit cycle sets (i.e., spiking states). In Fig. 4(a2), the two left plots (arrow α_3) correspond to unstable limit cycle sets and the right plots (arrow α_4) correspond to unstable equilibrium sets. When the post-synaptic input I is a small value, there exists the stable equilibrium set (arrow α_1) and it is surrounded by the unstable limit cycle set (arrow α_3). When I increases to I_1, the limit cycle set converges to the equilibrium set and the equilibrium set is unstabilized (arrow α_4). This bifurcation mechanism has qualitative similarities to a *subcritical Hopf bifurcation* [13].

In Fig. 4(b1), the two left plots (arrow α_5) correspond to stable limit cycle sets (i.e., spiking states) and the right plots (arrow α_6) correspond to stable equilibrium sets (i.e., resting states). In Fig. 4(b2), the plots (arrow α_7) correspond to unstable equilibrium sets. When the post-synaptic input I is a small value, there exists the unstable equilibrium set (arrow α_7) and it is surrounded by the stable limit cycle set (arrow α_5). When I increases to I_2, the limit cycle set converges to the equilibrium set and the equilibrium set is stabilized (arrow α_6). This bifurcation mechanism has qualitative similarities to a *supercritical Hopf bifurcation* [13].

In Fig. 4(c1), the left plots (arrow α_8) correspond to stable equilibrium sets (i.e., resting states) and the right plots

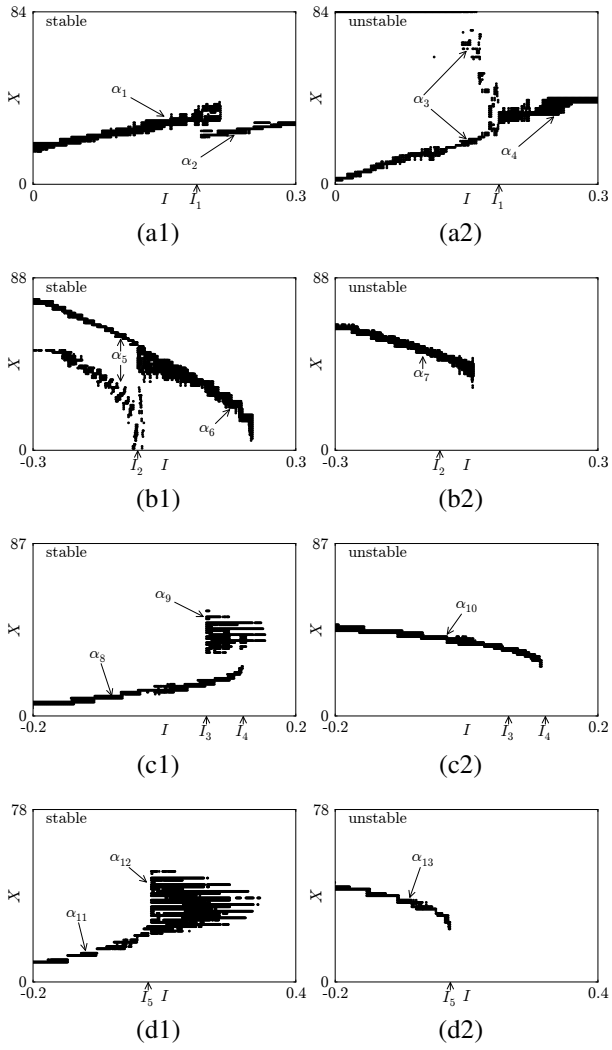

Figure 4: Bifurcation diagrams with for X respect to a post-synaptic stimulation I. (a1)–(d1) show the stable periodic points and (a2)–(d2) show the unstable periodic points. The bit lengths are $M = N = K = J = 64$. (a1)(a2) The parameters are $\mathbf{\Gamma} = (7, 0.3, 0.2, 3, 0.1, 64, 0.5, 0.3, 0)$. (b1)(b2) The parameters are $\mathbf{\Gamma} = (7, 0.3, 0.5, -2.53, -0.05, 64, -0.33, 0.3, -0.04)$. (c1)(c2) The parameters are $\mathbf{\Gamma} = (7, 0.3, 0.2, -0.5, 0.1, 64, 4, 0.37, 0.35)$. (d1)(d2) The parameters are $\mathbf{\Gamma} = (7, 0.3, 0.2, -0.5, 0.05, 64, 4, 0.25, 0.4)$.

(arrow α_9) correspond to stable limit cycle sets (i.e., spiking states). In Fig. 4(c2), the plots (arrow α_{10}) correspond to unstable equilibrium sets. When the post-synaptic input I is a small value, there exist the stable equilibrium set (arrow α_8) and the unstable equilibrium set (arrow α_{10}). When I increases to I_3, the two eqilibrium sets collide and disappear. This bifurcation mechanism has qualitative similarities to a *saddle-node bifurcation* [13]. When the post-synaptic input I is a large value, there exist the stable limit cycle (arrow α_9). When I decreases to I_4, the limit cycle set collides with the unstable equilibrium set (arrow α_{10}) and disappears. This bifurcation mechanism has qualitative similarities to a *saddle homoclinic orbit bifurcation* [13].

In Fig. 4(d1), the left plots (arrow α_{11}) correspond to stable equilibrium sets (i.e., resting states) and the right plots (arrow α_{12}) correspond to stable limit cycle sets (i.e., spiking states). In Fig. 4(d2), the plots (arrow α_{13}) correspond to unstable equilibrium sets. When the post-synaptic input I is a small value, there exist the stable equilibrium set (arrow α_{11}) and the unstable equilibrium set (arrow α_{13}). When I increases to I_5, the two eqilibrium sets collide and disappear. At the same instant, the stable limit cycle set (arrow α_{12}) appears. This bifurcation mechanism has qualitative similarities to a *saddle-node on invariant circle bifurcation* [13].

4. Conclusion

The *generalized asynchronous digital spiking neuron model* (ab. GDN) whose dynamics is described by the asynchronous cellular automaton is proposed, where the sensitivity of its vector field to the stimulation input is generalized. It has been shown that the GDN can exhibit various bifurcations observed in some standard ODE neuron models. These properties will be keys to reproduce responses of biological and model neurons. Future problems include: clarification of relationships between the parameters of the GDN and experimentally measurable parameters of biological neurons, development of an on-chip learning algorithm of the GDN, and development of a neuroscience-aware network of GDNs. The authors would like to thank Professor Toshimitsu Ushio of Osaka University for valuable discussions. This work is partially supported by the Center of Excellence for Founding Ambient Information Society Infrastructure, Osaka University, Japan, and KAKENHI (21700253).

References

[1] J. V. Arthur and K. A. Boahen, "Silicon-Neuron Design: A Dynamical Systems Approach," *IEEE Trans. on Circuits and Systems I*, vol. 58, no. 5, pp. 1034–1043, 2011.

[2] J. H. B. Wijekoon and P. Dudek, "Compact silicon neuron circuit with spiking and bursting behaviour," *Neural Networks*, vol. 21, no. 2-3, pp. 524–534, 2008.

[3] R. J. Vogelstein, U. Mallik, J. T. Vogelstein, and G. Cauwenberghs, "Dynamically reconfigurable silicon array of spiking neurons with conductance-based synapses," *IEEE Trans. on Neural Networks*, vol. 18, no. 1, pp. 253–265, 2007.

[4] H. Chen, S. Saï andghi, L. Buhry, and S. Renaud, "Real-Time Simulation of Biologically Realistic Stochastic Neurons in VLSI," *IEEE Trans. on Neural Networks*, vol. 21, no. 9, pp. 1511–1517, 2010.

[5] R. K. Weinstein, M. S. Reid, and R. H. Lee, "Methodology and Design Flow for Assisted Neural-Model Implementations in FPGAs," *IEEE Trans. on Neural Systems and Rehabilitation Engineering*, vol. 15, no. 1, pp. 83–93, 2007.

[6] T. Schoenauer, S. Atasoy, N. Mehrtash, and H. Klar, "Neuropipe-chip: A digital neuro-processor for spiking neural networks," *IEEE Trans. on Neural Networks*, vol. 13, pp. 205–213, 2002.

[7] J. W. Moore and F. Ramon, "On numerical integration of the hodgkin and huxley equations for a membrane action potential," *Journal of Theoretical Biology*, vol. 45, no. 1, pp. 249–273, 1974.

[8] H. Torikai, H. Hamanaka, and T. Saito, "Reconfigurable digital spiking neuron and its pulse-coupled network: Basic characteristics and potential applications," *IEEE Trans. on Circuits and Systems II*, vol. 53, no. 8, pp. 734–738, 2006.

[9] S. Hashimoto and H. Torikai, "A novel hybrid spiking neuron: Bifurcations, responses, and on-chip learning," *IEEE Trans. on Circuits and Systems I*, vol. 57, no. 8, pp. 2168–2181, 2010.

[10] T. Hishiki and H. Torikai, "A Novel Rotate-and-Fire Digital Spiking Neuron And its Neuron-like Bifurcations and Responses," *IEEE Trans. on Neural Networks*, vol. 22, no. 5, pp. 752–767, 2011.

[11] T. Matsubara and H. Torikai, "A novel asynchronous digital spiking neuron model and its various neuron-like bifurcations and responses," in *Proc. of International Joint Conference on Neural Networks*, 2011 (in press).

[12] E. M. Izhikevich, *Dynamical Systems in Neuroscience: The Geometry of Excitability and Bursting*. The MIT Press, 2006.

[13] Y. A. Kuznetsov, *Elements of Applied Bifurcation Theory*. Springer, 1995.